PREPARATION OF MAGNETIC SILICA NANOPARTICLES AS DRUG DELIVERY SYSTEMS BY USING SUPERCRITICAL CARBON DIOXIDE

Nerea Murillo-Cremaes[1], *Javier Saurina*[2], *Pascal Subra-Paternault*[3], *Anna Roig*[1*], *Concepción Domingo*[1*]
[1] *Institut de Ciència de Materials de Barcelona (CSIC), Campus de la UAB, Bellaterra, E-08193, Spain.*
[2] *Department of Analytical Chemistry. University of Barcelona, Martí i Franquès 1–11, Barcelona, E-08028, Spain.*
[3] *Université Bordeaux, CBMN UMR 5248, Bat B14 bis, Allée Geoffroy St Hilaire, 33600 Pessac, France*

ABSTRACT

The objective of the present work was to prove the utility of supercritical CO_2 (scCO2) to satisfy one of principal demands on the material science processing: the fabrication of functional nanostructured materials combining superior properties to be applied in pharmacy. In particular, we focus on the design of porous and magnetic silica nanoparticles for drug delivery applications. The unique properties that the supercritical fluids present, makes them especially suitable for pharmaceutical processing. In order to synthesize those particles, we used $scCO_2$ playing three different roles: first, as reaction medium to prepare iron oxide-silica nanospheres (less than 100 nm in size) by a novel sol-gel strategy. Secondly, it was used as solvent for a model drug (an anti-platelet agent named triflusal) to be impregnated in the porous silica matrix. Since these drug loaded particles exhibited a release profile in both acidic (pH=2, as stomach) and neutral (pH=7.4, as bloodstream) extremely fast, a biocompatible polymer was used to coat the spheres by precipitating it onto the silica surface in a third step assisted by $scCO_2$ as antisolvent. The resulting nanostructured material delivered the drug in a controlled and prolonged diffusion process.

INTRODUCTION

Pharmaceutical industry is now moving to the development of new formulations based on drug delivery systems with engineered biodistribution profiles to overcome traditional problems related to side effects, insufficient drug concentration at targeted sites, rapid metabolization or drug degradation. The use of nanoparticulate carriers to enhance the *in vivo* efficiency of active agents has been widely established during the past decade.[1][2] They ease a prolonged circulation after administration, increasing bioavailability and enhancing the percentage of unaltered active agent that reaches the damaged area. Nanoporous inorganic materials, such as silica (SiO_2) with several levels of sophistication in their architecture and/or composition have also been proposed as drug delivery devices.[3][4] Moreover, mesoporous silica magnetic nanocomposites are being studied for application in simultaneous diagnosis (magnetic resonance imaging) and therapy (hyperthermia and externally guided drug-delivery vehicles).[5][6]

Polymer coating of micro and nanoparticles is presently a widely used technique for powder processing in various important industries. In the particular case of controlled drug delivery, encapsulation of inorganic materials (among others) is used to modulate the release rate of the active pharmaceutical ingredient to the organism. Other advantages attained by coating are better dispersion and deagglomeration, as well as enhanced functionality when

coated with specific polymers such as polyethylenglycol[7][8], which gives amphiphilic character and prevent recognition by the immune system.

In the last years the unique properties of $scCO_2$ have been advantageously exploited both in innovative processes designing drug delivery systems[9][10] and in the industry of coating. Regarding the second one, CO_2 has a limited solvent strength for many polymers of interest. Hence, most of the work performed in coating using this fluid has been carried out by antisolvent methods.[11][12]

The replacement of organic solvents with $scCO_2$ results in an environmentally friendly option with a near-zero waste production. Moreover, CO_2 is an ideal processing medium because of its relatively mild critical conditions (31.1 ºC and 73.8 bar) and GRAS (generally recognized as safe) status. Both are important features for the pharmaceutical processing.[13]

MATERIALS AND METHODS

Preparation of iron oxide@silica nanoparticles (AP_{Fe}): magnetite nanoparticles (Fe_3O_4 NPs) were pre-synthesized by a modification of the method firstly described by Sun et al.[14] In a typical experiment, the following reactants were used as received: iron (III) acetylactonate ($Fe(acac)_3$, 97%), 1,2-hexadecanediol (90%), oleylamine (70%), benzyl acohol (99%), all of them purchased from Aldrich, oleic acid acquired from Scharlab, hexane (≥ 98.5%) and ethanol (96% v/v) from Panreac. The resulting particles are 7 nm of mean diameter, with narrow particle size distribution (usually < 20%) and they remain stable in hexane for months. Nanoparticles are superparamagnetic at room temperature. Coating of those particles with silica to prepare AP_{Fe} naonparticles was done combining sol-gel hydrolysis and condensation of a silicon precursor and supercritical evacuation of the solvent inside an autoclave. Typically, initial reagents with a mass composition TMOS (tetramethylorthosilicate, 98%, Aldrich)/H_2O/acetone (QP, Panreac)/Fe_3O_4/hexane 0.92/0.22/95.6/0.04/3.19 wt. % were placed in a Pyrex vessel at ambient conditions; the TMOS/H_2O molar ratio was kept fixed at 0.5 and the acetone/hexane volume ratio at 60. The vessel was then introduced in the 2.5 litres supercritical reactor and the pressure inside the reactor was increased up to 50 bar using carbon dioxide (CO_2, 99.995 wt%, Carburos Metálicos, Spain). Afterwards, temperature was raised up to 250ºC with the corresponding increase of pressure up to 250 bar. The final P and T values were over the critical point of any possible CO_2/acetone solvent mixture (P_c (max) = 120 bar and T_c (max) = 235ºC). After a given residence time at supercritical conditions, the system was depressurized up to 150 bar (still supercritical conditions) and fresh CO_2 was circulated for one hour with a flow of 0.5 kg_{CO2}/h and another hour at 1.5 kg_{CO2}/h. The circulation of clean CO_2 serves to drag out of the vessel the unreacted silicon precursor and thus, minimize the necking formation between the particles. Finally, the autoclave was depressurized and cooled down to room temperature. Each experiment took eight hours. The resulting material was a dry powder homogenously distributed around the reactor walls.

Impregnation of AP_{Fe} with a drug: 2-Acetyloxy-4-(trifluoromethyl) benzoic acid (triflusal, Trf) was used as a model drug to be impregnated. The metabolite of Trf (4-(trifluoromethyl)salicylic acid, HTB) was also analyzed to follow the evolution of the drug degradation with time. Both were kindly donated by Uriach S.A., Spain. Impregnation process in $scCO_2$ was performed in a batch mode equipment described elsewhere.[15] The autoclave (100 mL) was charged with drug and particles in a weight ratio of *ca.* 1:2. AP_{Fe} particles were first dehydrated by heating in a tubular oven (Carbolite 3216) at 300 ^oC for 2 h under a flow of nitrogen. The powder was then wrapped in a cylinder made of 0.45 μm pore

filter paper, and added to the reactor maintaining a physical separation from the drug of 2-3 cm. The reactor was filled with pressurized CO_2 up to 200 bar and heated to 45 ºC. In all the experiments performed, the amount of commercial Trf was added in excess ensuring saturation of the $scCO_2$ phase. In a typical run, the charged autoclave was magnetically stirred at 300 rpm during 6 h. This impregnation approach is reproducible and it has been demonstrated by repeating the experiments at least three times and obtaining similar results. The resulting material was labeled as $Trf@AP_{Fe}$.

Polymer coating of Trf@APFe nanoparticles: Eudargit® RL 100 (Evonik Rohm Pharma Polymer, Degussa) was the polymer of choice. It is non-toxic, biocompatible and highly soluble in acetone but insoluble both in CO_2 and in water. First, an acetone suspension with $Trf@AP_{Fe}$ (5 $mgmL^{-1}$), polymer (20 m gmL^{-1}) and an extra amount of Trf (6.5 $mgmL^{-1}$) was prepared. SAS semicontinuous approach was employed for coating. The equipment is fully described elsewhere.[16] The heated high pressure autoclave (30 ºC) was first filled with CO_2 at a pressure of 90 bar and, then, a volume of the acetone suspension (just sonicated for 15 minutes) was sprayed into the vessel at a flow rate of 1.5-2.0 mL min^{-1}. A capillary nozzle (180 µm diameter) was used to deliver the suspension. Liquid CO_2 was continuously pumped to the vessel at a rate of 15-25 g min^{-1} during the injection and afterwards for 1 h to wash the obtained product. Coated materials were recovered on a 5 µm filter overtopped by two membranes of 0.22 µm placed at the bottom of the autoclave. The resulting material was named as $EudAP_{Fe}$.

Characterization: The obtained materials were characterized by different techniques. *Transmission electron microscopy* (TEM) was performed in a JEOL JEM-1210 microscope. Chemical Analysis (concretely *Inductively coupled plasma combined with mass spectroscopy* (ICP-MS) was applied to obtain the Si/Fe mass ratio. *Magnetic measurements* were done by measuring magnetization vs. applied magnetic field at 298 K with a superconducting quantum interference device (SQUID) magnetometer (Quantum Design MPMS5XL). *Nitrogen adsorption/desorption* data (by applying the BET and BJH methods) were taken at 77 K using an ASAP 2000 surface area analyzer (Micromeritics Instrument Corporation) after degasification under vacuum for 24 h at 300ºC to remove the adsorbed species. *Relaxivity measurements*: T1 and T2 relaxation times were measured using an inversion-recovery pulse sequence with a Bruker Minispec (Bruker Analytics, North Bellirica, MA) at 37 ºC and 0.47 T (20 MHz). *Fourier transform infrared spectroscopy* (FTIR) was performed in a Perkin Elmer Spectrum One instrument. *X-ray diffraction* (XRD) was done with a Siemens D5000 X-ray powder diffractometer using Cu Kα incident radiation. An equipment of *high performance liquid chromatography* (HPLC) described elsewhere[17] was employed for different purposes: study of the drug release profiles in both acidic medium (pH = 2, 0.01M HCl simulating the stomach pH) and basic one (pH = 7.4, a mixture of phosphate salts at 0.01M, as the blood plasma pH), obtaining of the drug amount entrapped in AP_{Fe} particles after the impregnation and coating processes (both the Trf and the HTB contributions were considered) and to know the hydrolysis degree of Trf. The solid powder was immersed in the different media at 37 ºC and stirring at 60 rpm.

RESULTS

The synthesized iron oxide@silica nanoparticles were composed by clusters of magnetite nanospheres coated by a broad layer of silica. Those composite particles were 65 nm in mean diameter with a 23% of polydispersity (see fig. 1). Magnetite (Fe_3O_4) content was found to be 9.8% from the total mass while the silica (SiO_2) percentage was 72.6%. The fact

that those amount were not equal to 100% was attributed to the presence of unreacted materials or impurities.

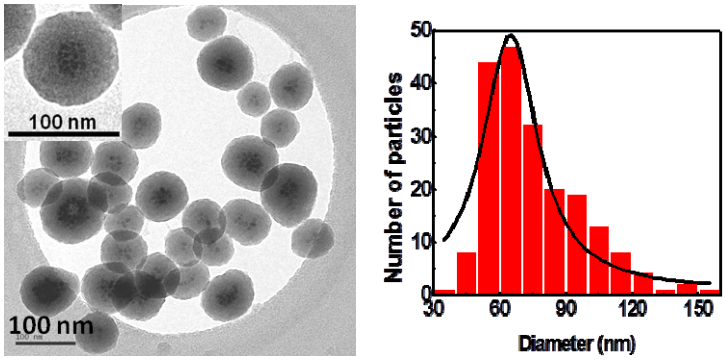

Figure 1. TEM micrograph of the obtained iron oxide@silica nanoparticles (AP_{Fe}) and size histogram fitted to a Gaussian distribution.

The particles presented a superparamagnetic behavior with high magnetization saturation (approx. 60 emu/g Fe_3O_4 at 300K), with no hysteresis loop as it can be observed in fig. 2. This value is comparable to the one of the bulk material. These results confirm that there are no strong magnetic dipolar interactions between the particles forming the nucleus and that the supercritical drying has not induced sintering or particle growth. At room temperature, these two situations could induce a magnetic clump in the presence of an external magnetic field which wouldn't be helpful for the biomedical applications targeted since one of the interesting advantages of superparamagnetic particles is that they are only magnetized in the presence of an external magnetic field, avoiding agglomeration and possible embolization of capillary vessels. In figure 2, the magnetic properties of the powder are clearly seen when it is close to a magnet.

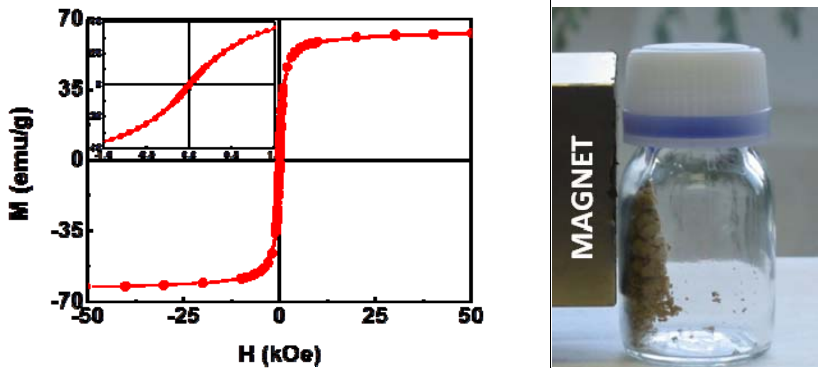

Figure 2. Magnetization vs. applied field of AP_{Fe} paticles measured at room temperature (300 K) and a photograph of the magnetic powder formed by those particles being attracted by a 0.5 T magnet.

Previous studies in our group showed that those particles are good negative contrast agents for MRI, with relaxometry values above 300 $mmol^{-1}s^{-1}$.[18] We also demonstrated that the monodispersed magnetite NPs, previous to the silica coating, were good positive contrast agents[19] (see table 1).

The mean pore size of the particles fitted in the micro range (pore diameters < 2 nm) and the N_2 adsorption/desorption isotherm also confirmed this observation being of type I according to the IUPAC classification[20] (results not shown). Particles presented a surface area of 160 m^2g^{-1}. It is worth to mention that this porosity was achieved without using any surfactant of porogenic agent.

Table 1. Relaxometry values for magnetite and composite APFe nanoparticles as T1 and T2 contrast agents related with their mean sizes.

Sample	Size (nm)	r_1 (mmol^{-1} s^{-1})	r_2 (mmol^{-1} s^{-1})	r_2/r_1
Fe_3O_4 NPs	5	17.6	35.7	2.03
AP_{Fe} NPs	160	< 0.2	326	> 500

Once the composite particles were impregnated with triflusal, the presence of the drug was proved by FTIR. Figure 3 shows infrared spectra of both the therapeutic agent and its metabolite in aqueous medium and of the impregnated Trf@AP_{Fe} nanoparticles. Characteristic absorption peaks corresponding to vibration of the carbonyl C=O group of Trf and HTB was found in the impregnated powder (around 1703 cm^{-1}).

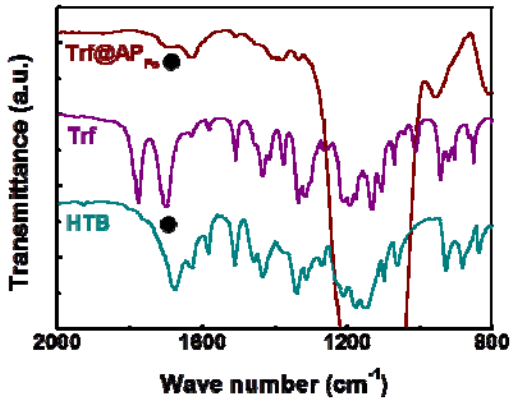

Figure 3. Infrared spectra of the drug (Trf) and its metabolite in water (HTB) and of the drug impregnated composite nanoparticles (Trf@AP_{Fe}). The round symbols (●) mark the peaks of C=O groups coming from the drug.

XRD was used to assess the occurrence or the absence of crystalline arrangement for the entrapped drug. Spectra of the therapeutic agents and the impregnated particles are exhibited in figure 4. Triflusal could be readily identified by its two most intense peaks at 2θ = 19.38 and 25.92º, while HTB displayed two intense peaks at 2θ = 16.64 and 24.48º. Concerning AP_{Fe} matrix, the same silica band appeared together with the characteristics (220) and (311) peaks of magnetite at 2θ = 30 and 36 º. Diffraction peaks of the Trf (or HTB) crystalline form did not appear in the XRD patterns of the prepared composite products, in which only the amorphous hill of the matrix was clearly observed, thus indicating that the drug did not crystallize during supercritical impregnation.[21]

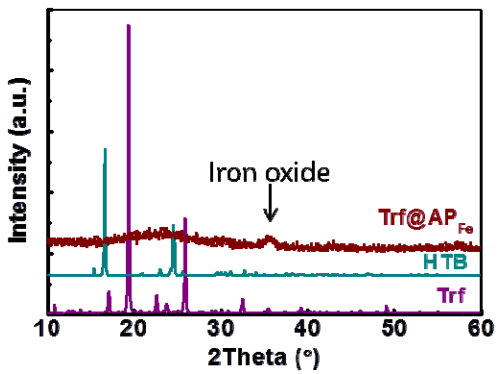

Figure 4. XRD spectra of the drug Trf, its metabolite HTB and drug loaded particles (Trf@AP_{Fe}).

We synthesized other nanostructured silica matrices for the drug, such as aerogel (AG) and microporous silica sub-micron particles (AP). The drug release kinetics in different media for the three systems was studied by HPLC as explained above. Figure 5 graphs the results obtained in acidic medium (similar to those obtained in basic medium). The particulate matrices deliver the drug almost immediately; the most part is released in the first minute. The discharge from the AG is slower but also fast, with the 90% of the drug delivered in 25 minutes. Considering that the whole amount of the drug is discharged after 2 hours, 17% is registered for the AG, while around 3 and 4% for the particles. This kind of materials has potential applications in local injections, where their magnetic properties could fix them in the desired area ant he drug solubility needs to be enhanced. Moreover, AP_{Fe} particles size allow an easy excretion.

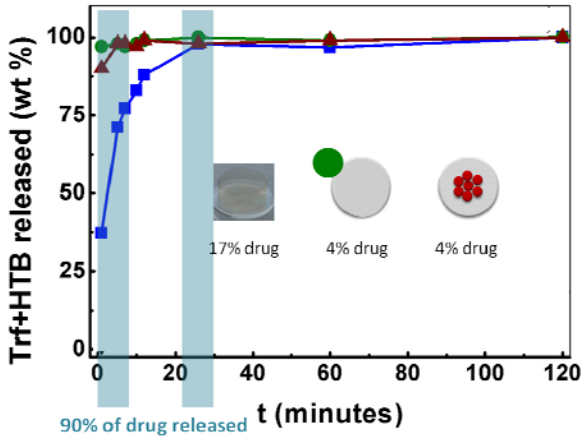

Figure 5. Drug release profile of different silica-based matrices impregnated with triflusal: aerogel (Trf@AM), silica particles (Trf@AP) and the composite nanospheres (Trf@AP_{Fe}).

The SAS coating process over the drug loaded particles produced spheres embedded in a polymer (see fig. 6a and its inset to identify a smaller aggregate of coated particles), which was partially eliminated with the proper solvent (by means acetone, ethanol, methanol, etc…) giving place to almost individually coated particles, as it is shown in fig. 6b. The polymer coating can be observed in the inset as a thin layer that covers and attach the nanoparticles between them. In these images, it can be observed that the thin layer of polymer was also attaching individual particles together.

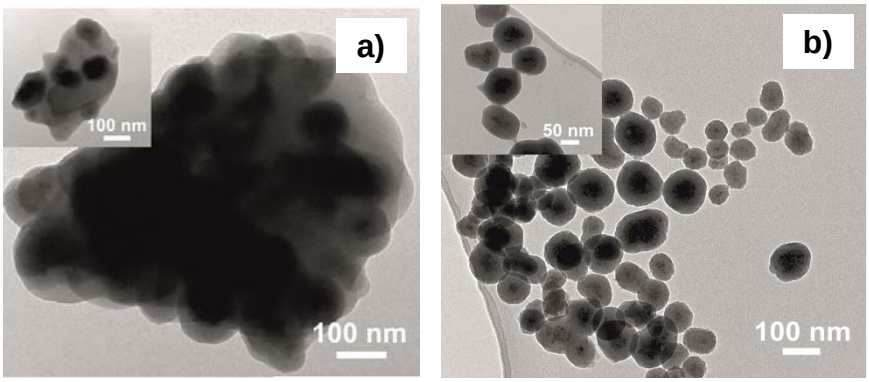

Figure 6. TEM images of: (a) $EudAP_{Fe}$ sample (the inset is magnified picture of the same sample) and (b) $EudAP_{Fe}$ sample rinsed with methanol. In the inset a closer look of these rinsed nanoparticles is seen.

The most distinctive band in the IR spectrum of Eudragit was the C=O vibration appearing at *ca.* 1725 cm^{-1}. Moreover the asymmetric and symmetric alkyl bending modes appeared as a shoulder at *ca.* 1480 cm^{-1} and as two peaks at *ca.* 1445 and 1385 cm^{-1}, respectively (see fig. 7). Those signals were also detected in coated particles. The presence of Trf in the coated matrices was difficult to assess, due to the low percentage of the drug in the samples in comparison with the other components.

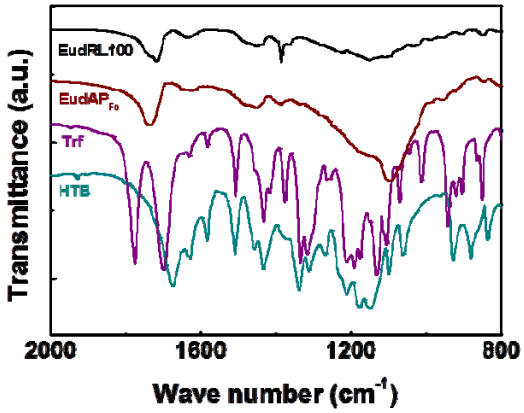

Figure 7. Infrared spectra of the drug (Trf), its metabolite in water (HTB), the coated composite particles EudAPFe and the polymer Eudragit® RL100.

The drug release profile of $EudAP_{Fe}$ changed significantly from the one obtained with particles $Trf@AP_{Fe}$ prior to polymer coating. While the uncoated material exhibited a extremely fast release with the 90% of the drug delivered within the first minute (fig. 5), the hybrid material with the polymer presented a sustained release in which the 90% is delivered after two hours and a half (see figure 8).

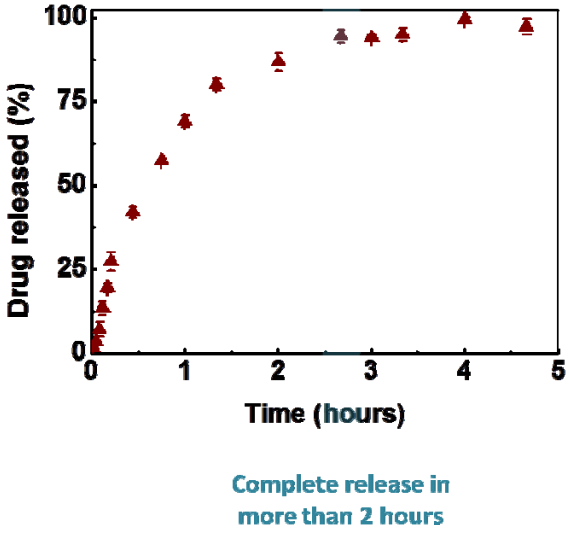

Figure 8. Drug release profile of $EudAP_{Fe}$ particles.

CONCLUSIONS

Supercritical carbon dioxide has been successfully employed to withdrawn different processes in the preparation of drug loaded magnetic silica nanospheres for controlled drug delivery. First, a one-pot and one-step synthesis method was performed to obtain spherical nanocomposite particles, with narrow particle size distribution and tuneable size. Those particles were later impregnated with a model drug in molecular form by dissolution in $scCO_2$. This system showed a extremely fast release of the therapeutic agent with potential applications in local injections. Finally, more complex materials were prepared by coating, in presence of CO_2, the drug loaded composite nanoparticles with a biopolymer. This leads on a improved control over the release profile.

REFERENCES

[1] Torchilin, V.P., Advanced Drug Delivery Reviews, Vol. 58, **2006**, p. 1532.
[2] Peer, D., Karp, J.M., Hong, S., Farokhzad, O.C., Margalit, R., Langer, R., Nature Nanotechnology, Vol. 2, **2007**, p. 751.
[3] Qian, K.K., Bogner, R.H., Journal of Pharmaceutical Sciences, Vol. 101, **2012**, p. 444.
[4] He, Q., Shi, J., Journal of Materials Chemistry, Vol. 21, **2011**, p. 5845.
[5] Chen, I., Hangrong, C., Seng, D., Tian, Y., Chen, F., Feng, J., Shi, J., ACS Nano, Vol. 4, **2010**, p. 6001.
[6] Liong, M., Angelos, S., Choi, E., Patel, K., Stoddart, J.F., Zink, J.I., Journal of Materials Chemistry, Vol. 19, **2009**, p. 6251.
[7] Marre, S., Cansell, F., Aymonier, C., Langmuir, Vol. 24, **2008**, 252.
[8] Orts-Gil, G., Natte, K., Thiermann, R., Girod, M., Rades, S., Kalbe, H., Thünemann, A.F., Maskos, M., Österle, W., Colloid and Surfaces. B: Biointerfaces, Vol. 108, **2013**, p. 110.
[9] Martín, A., Cocero, M.J., Advanced Drug Delivery Reviews, Vol. 60, **2008**, p. 339.
[10] Yasuji, T., Takeuchi, H., Kawashima, Y., Advanced Drug Delivery Reviews, Vol. 60, **2008**, p. 388.
[11] Cansell, F., Aymonier, C., Journal of Supercritical Fluids, Vol. 47, **2009**, p. 508.
[12] Seremeta, K.P., Chiappetta, D.A., Sosnik, A., Colloid and Surfaces B: Biointerfaces, Vol. 102, **2013**, p. 441.
[13] Domingo, C., Saurina, J., Analytica Chimica Acta, Vol. 744, **2012**, p. 8.
[14] Sun, S., Zeng, H., Robinson, D.B., Raoux, S., Rice, P.M., Wang, S.X., Li, G., Journal of American Chemical Society, Vol. 126, **2004**, p. 273.
[15] López-Periago, A., Argemí, A., Andanson, J.M., Fernández, V., García-González, C.A., Kazarian, S.G., Saurina, J., Domingo, C., Journal of Supercritical Fluids, Vol. 48, **2009**, p. 56.
[16] García-González, C.A., Vega-González, A., López-Periago, A.M., Subra-Paternault, P., Domingo, C., Acta Biomaterialia, Vol. 5, **2009**, p. 1094.
[17] Argemí, A., López-Periago, A., Domingo, C., Saurina, J., Journal of Pharmaceutical and Biomedical Analysis, Vol. 46, **2008**, p. 456.
[18] Taboada, E., Solanas, R., Rodríguez, E., Weissleder, R., Roig, A., Advanced Functional Materials, Vol. 19, **2009**, p. 2319.
[19] Taboada, E., Rodríguez, E., Roig, J., Oró, J., Roch, A., Muller, R.N., Langmuir, Vol. 23, **2007**, p. 4583.
[20] Sing, K.S.W., Everett, D.H., Haul, R.A.W., Moscou, L., Pierotti, R.A., Rouquerol, J., Siemieniewska, T., Pure and Applied Chemistry, Vol. 57, **1985**, p. 603.
[21] Murillo-Cremaes, N., López-Periago, A.M., Saurina, J., Roig, A., Domingo, C., Journal of Supercritical Fluids, Vol. 73, **2013**, p. 34.